

H₂ shocks and mass accretion rate in high mass young stellar objects (HMYSOs)

Paolo Persi^{*†}

INAF/IAPS, Roma, Italy

E-mail: paolo.persi@iaps.inaf.it

Mauricio Tapia

UNAM, Instituto de Astronomia, Ensenada, Mexico

We have observed in the near and mid infrared a sample of high mass young stellar objects in order to understand the mechanisms of formation of these sources. In particular we have searched for the H₂ shocks. From their spectral energy distributions obtained combining observations at different wavelengths, we have obtained the physical parameters such as the mass accretion rate, the disk mass and the luminosity of these source.

*Accretion Processes in Cosmic Sources - APCS2016
5-10 September 2016,
Saint Petersburg, Russia*

*Speaker.

†A footnote may follow.

1. Introduction

Jets from young stellar objects (YSOs) are important signatures of star formation in molecular clouds. The molecular hydrogen emission H_2 S(1-0) at $2.121\mu\text{m}$ is a good tracer in detecting jets in form of knots. In low-mass YSOs, these jets are a common phenomena, while in high-mass protostars the jets are relatively rare and, usually, they are distant and highly embedded in their parental clouds. A search for H_2 jets in moderate and high mass young stellar objects has been obtained by [1]

In this paper we extend the search of H_2 jets in a sample of 10 high mass young stellar objects which characteristics are reported in Section 2. In addition ground based mid-IR images have been obtained in order to complete the study of this sample. Finally combining observations from near-IR to millimeter wavelengths, we have derived the spectral energy distribution (SED) of these sources. A detailed analysis of the SEDs allows to determine the parameters such as mass accretion rates of the YSOs

The observations are described in Section 3, while in Section 4 we discuss in details the properties of the detected sources. Finally the conclusions are given in Section 5.

2. Properties of the observed sample

Our observed sample reported in Table 1, consists of 10 IRAS sources associated with ammonia NH_3 cores [2], methanol and water masers ([3, 4]). According to their [25-12] and [60-12] colors these sources are classified as *High* sources (H), which have $[25-12] \geq 0.57$ and $[60-12] \geq 1.3$ and *Low* sources (L) . with $[25-12] \leq 0.57$ or $[60-12] \leq 1.3$ by [4]. In addition these sources have been observed in sub-millimeter, millimeter and in the radio continuum ([5],[6],[7]). The presence of CO outflow has been detected in most of these sources [8].

All these observations indicate the presence of high-mass young stellar objects in our sample.

3. Observations

3.1 Near-Infrared images

Near-infrared images through narrow-band H_2 ($\lambda_0 = 2.122 \mu\text{m}$, $\Delta\lambda = 0.032 \mu\text{m}$) and K_{cont} ($\lambda_0 = 2.270 \mu\text{m}$, $\Delta\lambda = 0.034 \mu\text{m}$) filters, as well as through standard broad-band JHKs filters, were collected on the nights of 2008 July 13 and 15, and 2008 November 14,15 using the Near Infrared Camera Spectrometer (NICS) attached to the 3.58 m Telescopio Nazionale Galileo (TNG) at the Observatorio del Roque de los Muchachos on La Palma island. The NICS has a HgCdTe Hawaii 1024×1024 array and was used in the SF (small field) configuration that provides a scale of 0.13arcsec/pixel.

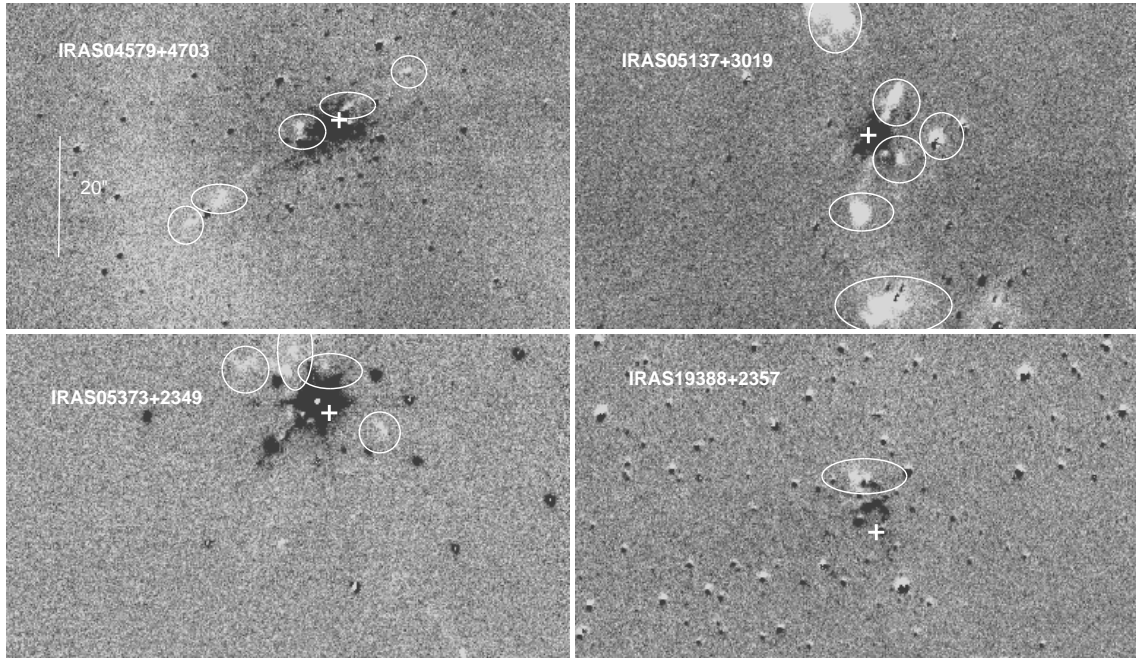
All images were calibrated with the photometric standard stars ([9],[10]). The measured FWHM of the point-spread function (PSF) is between 0.6arcsec and 0.8arcsec. *JHKs* photometry was obtained using DAOPHOT [11] within IRAF in the standard way, with an aperture of 1arcsec.

3.2 Ground based mid-Infrared images

Mid-infrared images at 8.9, 9.9, 12.7, and $18.7 \mu\text{m}$ of the sources of Table 1 were taken on the night of 2006 November 7 with the mid-infrared camera CID [12] on the 2.1 m telescope of the

Table 1: List of the observed HMYSOs.

Source	IRAS	Type	$\alpha(2000)$			$\delta(2000)$			D (Kpc)	L L_{\odot}	H_2
			h	m	s	°	'	"			
Mol 7	04579+4703	H	05	01	39.7	47	07	23	2.47	$3.91 \cdot 10^3$	Y
Mol 8	05137+3919	L	05	17	13.8	39	22	20	11.50	$2.25 \cdot 10^5$	Y
Mol 12	05373+2349	L	05	40	24.1	23	50	53	1.17	$4.70 \cdot 10^2$	Y
Mol 15	06056+2131	H	06	08	40.5	21	31	02	1.50	$5.83 \cdot 10^3$	Y
Mol 83	18566+0408	H	18	59	10.0	04	12	15	6.76	$1.02 \cdot 10^3$	N
Mol 98	19092+0841	L	19	11	37.4	08	46	30	4.48	$9.20 \cdot 10^3$	N
G45.07+0.13	19110+1045	H	19	13	22.6	10	50	53	9.70	$1.42 \cdot 10^6$	N
Mol 110	19388+2357	H	19	40	59.4	24	04	39	4.27	$1.48 \cdot 10^4$	Y
Mol 143	22172+5549	L	22	19	09.2	56	05	02	2.40	$1.80 \cdot 10^3$	Y
G111.24-0.76	23139+5939	H	23	16	09.3	59	55	23	4.80	$2.50 \cdot 10^3$	N

**Figure 1:** H_2 images of four IRAS sources. The detected knots are indicated with ellipses, while the IRAS position is marked with a symbol (+).

Observatorio Astronómico Nacional at San Pedro Mártir, Baja California, Mexico. This camera is equipped with a Rockwell 128×128 pixel Si:As BIB detector array that delivers an effective scale of 0.55 arcsec/pix. The images were taken in the standard chop-nodding mode to remove the sky and telescope emission background. The standard stars α Lyr, β Peg, β And, γ Aql, and μ Cep were observed before and after the programme source at similar air-masses for flux calibration and to measure the point-spread function (PSF) at each wavelength. These values ranged from about 1.6 to 1.8 arcsec (FWHM) at the shorter wavelengths, to 2.6 arcsec at $18.7 \mu\text{m}$.

4. Discussion

4.1 Search for H₂ jets

In order to search for H₂ shocks, we have subtracted from the images taken with the H₂ filter the Kc continuum images. From the analysis of these subtracted images we found H₂ emission from six IRAS sources of our observed sample (see Tab.1) Fig.1 show H₂ subtracted images relative to four IRAS sources with the detected H₂ jets.

Six H₂ knots were detected around the positions of IRAS 04579+4703(Mol 7). Five of these knots are aligned along NW-SE direction. The outflow length > 29.5 arcsec and the direction is approximately 125.5deg(E-N) similar to that found by [1]. Two more H₂ jets are outside this direction. This outflow is consistent with that observed in ¹²CO(2-1) line [13]

More complex appears the H₂ emission in IRAS 05137+3019. At least two H₂ jets are present powered by two different HMYSOs (see Fig.1) - This is well illustrated by [14].

As appears in Tab.1 the detection of the H₂ jets is independent from the type of the IRAS source.

4.2 Characteristics of the sources powered the H₂ jets

We have obtained *JHKs* aperture photometry within a radius of 10 arcsec centered on the IRAS sources to derive the characteristics of the young stellar objects responsible for the observed H₂ jets. In the next subsections we will discuss individually the characteristics of these sources derived from an analysis of the SEDs comparing the observed fluxes with the model of [17]. Particularly important is the derived values of mass accretion rates of these HMYSOs.

4.2.1 IRAS 04579+4703(Mol 7)

IRAS 04579+4703 is a young high-mass stellar object with associated a radio source detected at 1.3 and 3.6 cm, with 7mm and 1.2mm emission [15]. H₂O maser emission was detected from this source by several investigators (i.e. [16]). A dense core was observed towards this region in NH₃ emission by [2] that renamed this source as Mol 7. The spatial coincidence of the millimeter peak with the centimeter source suggests that the underlying massive star is in a very young evolutionary stage, not having pushed away the surrounding material yet.

Figure 2 illustrates our *JHKs* three-color image of Mol 7. At the position of the IRAS source and coincident with the mm continuum emission, we have detected a source with a strong near-IR excess (H-Ks)= 3.47. This source has been detected in the mid-IR until 18.7 μm.(contours in Fig.2). Combining the flux densities from near-IR up to millimeter wavelengths, we have obtained the spectral energy distribution (SED) of this source shown in Fig. 3(*Left panel*). In order to derive the physical parameters of this source, the SED has been fitted with the infalling envelope+disc+central source radiation transfer model [17] by using the fitting tool [18]. The derived parameters relative to the best fit are reported in Table 2. It is very difficult determine the errors of these parameters as reported also by [18].

4.2.2 IRAS 05137+3919(Mol 8)

IRAS 05137+3919 also known as Mol 8 from the catalogue of [2], was detected at sub-mm, millimeter and in the radio at 3.6cm with VLA by [6]. Our color-coded *JHKs* image of this source

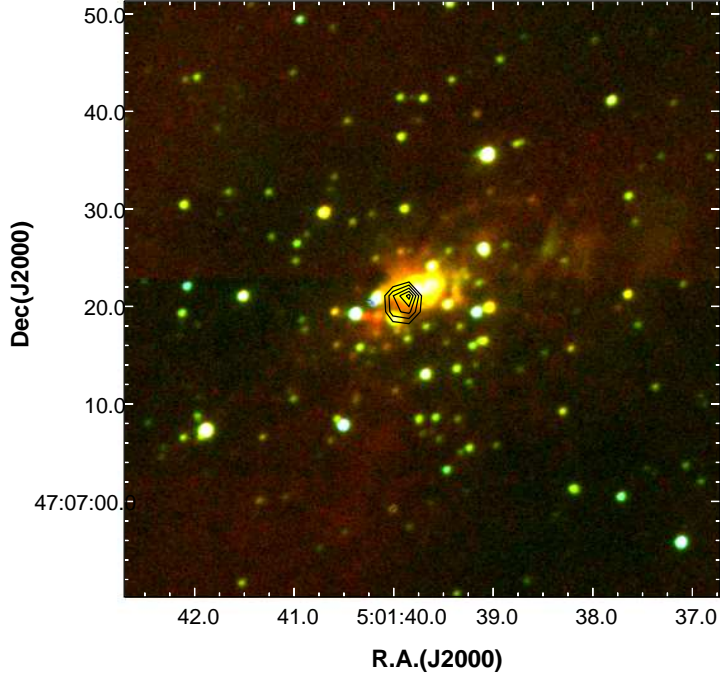


Figure 2: *JHKs* true color image made from *J*(blue), *H*(green) and *Ks* (red) images of IRAS 04579+47.03(Mol 7). The contours represent the observations at $18.7 \mu\text{m}$

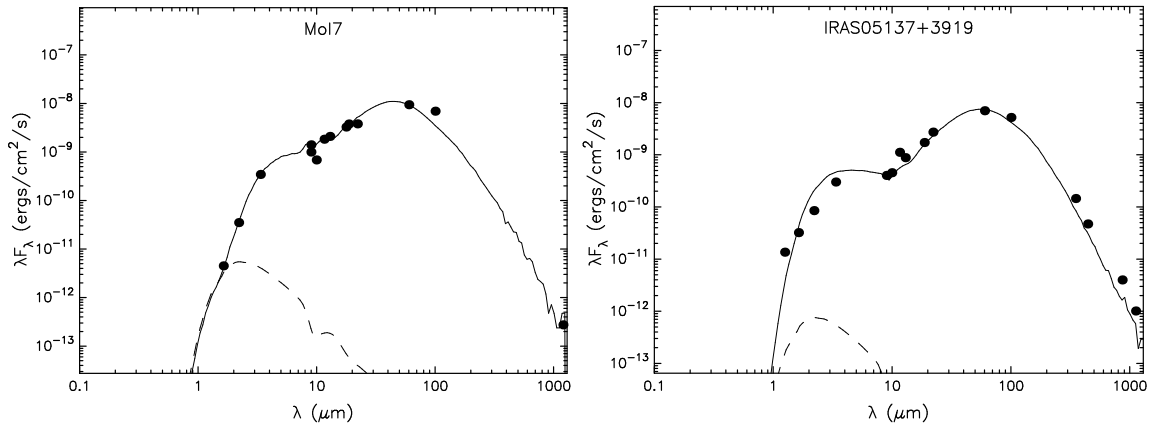


Figure 3: *Left panel:* Spectral energy distribution (SED) of IRAS 04579+4703(Mol 7).*Right panel:* SED of IRAS05137+3919(Mol 8).In both the diagrams the best-fit models of the SED derived from fitting tool [17] is over-plotted as solid line.

Table 2: Physical parameters of the protostellar objects Mol 7, Mol 8, Mol 12A and Mol 110, derived from model [17].

Parameters	Mol 7	Mol 8	Mol 12A	Mol 110
Stellar Mass (M_{\odot})	8.14	19.8	8.01	12.9
Stellar Temperature (K)	22927	35202	8000	12262
Envelope Accretion Rate (M_{\odot}/yr)	$1.1 \cdot 10^{-4}$	3.510^{-3}	5.610^{-4}	3.6010^{-3}
Envelope Cavity Angle (deg)	42.6	36.3	30	25.1
Disk Mass (M_{\odot})	6.7610^{-3}	1.4410^{-2}	6.1210^{-3}	1.4910^{-1}
A_V	23	20	23	42
L_{bol} (L_{\odot})	3.110^3	$9.2 \cdot 10^3$	$4.6 \cdot 10^3$	1.1310^4

is reported in Fig.4. The IRAS source is coincident with a near-IR source showing a near-IR excess and with a point like mid-IR source detected until $18.7 \mu\text{m}$. The SED of Mol 8 obtained combining the observations at different wavelengths is shown in the *Right panel* of Fig.3. As for the previous sources we have derived the physical parameters for this source reported in Table 2. Finally our observations show the presence of a young stellar cluster around the IRAS source. This cluster could be responsible for the complex H_2 emission observed in Mol 8 (see Fig.1).

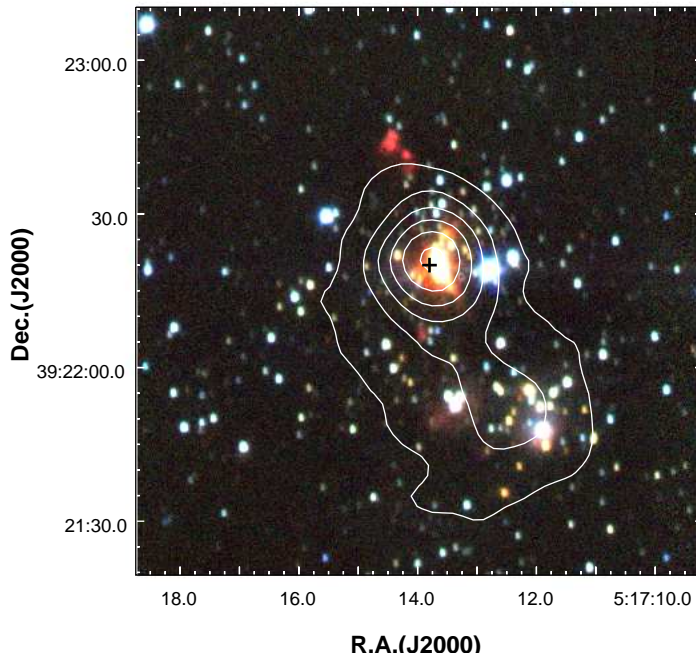


Figure 4: *JHKs* true color image made from J(blue), H(green) and Ks (red) images of IRAS 05137+3919 (Mol 8). The contours represent the mm observations. The position of the IRAS source is marked with a symbol (+).

4.2.3 IRAS 05373+2349(Mol 12)

This source is associated with ammonia emission from gas with a kinetic temperature of 21.2 K

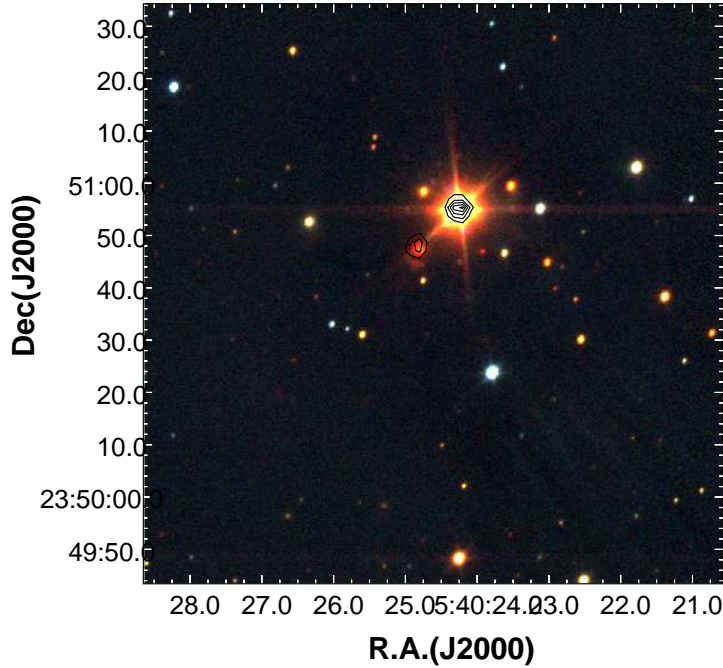


Figure 5: *JHKs* true color image made from *J*(blue), *H*(green) and *Ks* (red) images of IRAS 05373+2349 (Mol 12). The contours represent our 12.7 μm observation.

and has been renamed Mol 12 [2]. Radio and millimetre observations detected IRAS 05373+2349 at 3.6 cm and 3.4 mm respectively[7]. The radio emission is faint (0.70 ± 0.04 mJy at 3.6 cm) and is thought to arise from an ionized wind. Sub-mm and mm observations at 0.35 mm, 0.45 mm, 0.8 mm, 1.1 mm, 1.3 mm and 2.0 mm were carried out by [6]. The continuum-subtracted H_2 image obtained by [1] shows several faint emission features (at least six) centered around a bright object with near-IR excess, similar to our observations of Fig.1. It is noteworthy that the H_2 knots are roughly aligned in the direction of the outflow mapped in CO([8]) .

Figure 5 illustrates the *JHKs* color coded image of Mol 12. Two very red sources have been detected in the near and mid-IR with a prominent IR excess. One here named Mol 12A is very bright and coincides with the IRAS source. The second Mol 12B lies approximately 8 arcsec south-east of the IRAS source. We have build the SED of Mol 12A combining our measured fluxes in the near and mid-IR with sub-millimeter and millimeter observations (see Fig.6 (*Left panel*)) . The derived parameters for this source are shown in Table 2.

4.2.4 IRAS 19388+2357(Mol 110)

IRAS 19388+2357 is associated with H_2O maser emission [4], a radio source[5] and dense molecular gas traced in NH_3 by [2] who renamed as Mol110. Methanol maser was also detected from this source [19]. A CO outflow has been detected by [8]. The centroid of this CO emission is approximately 29 arcsec south of the IRAS position. Finally a dense core at 1.2mm with a mass

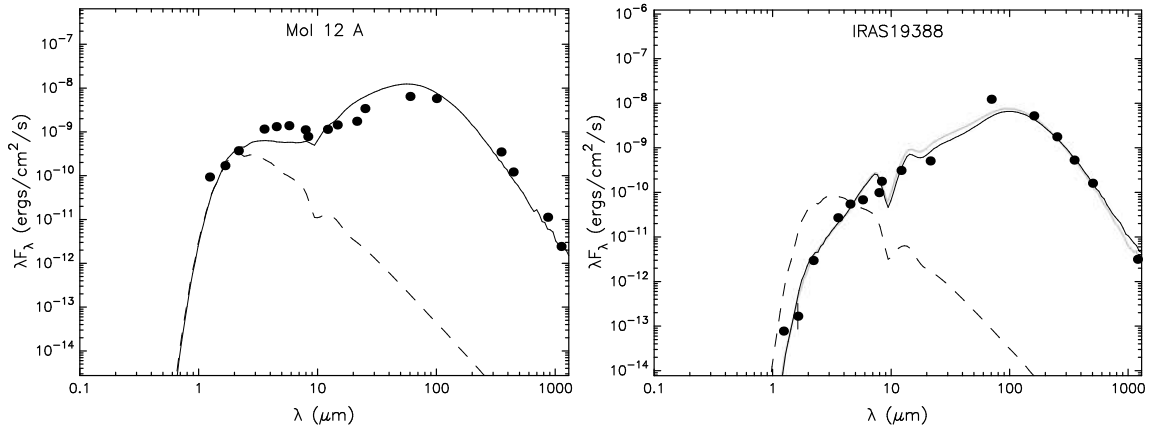


Figure 6: *Left panel:* Spectral energy distribution (SED) of IRAS 05373+2349(Mol 12A).*Right panel:* SED of IRAS 19388+2357(Mol 110).In both the diagrams the best-fit models of the SED derived from fitting tool [17] is over-plotted as solid line.

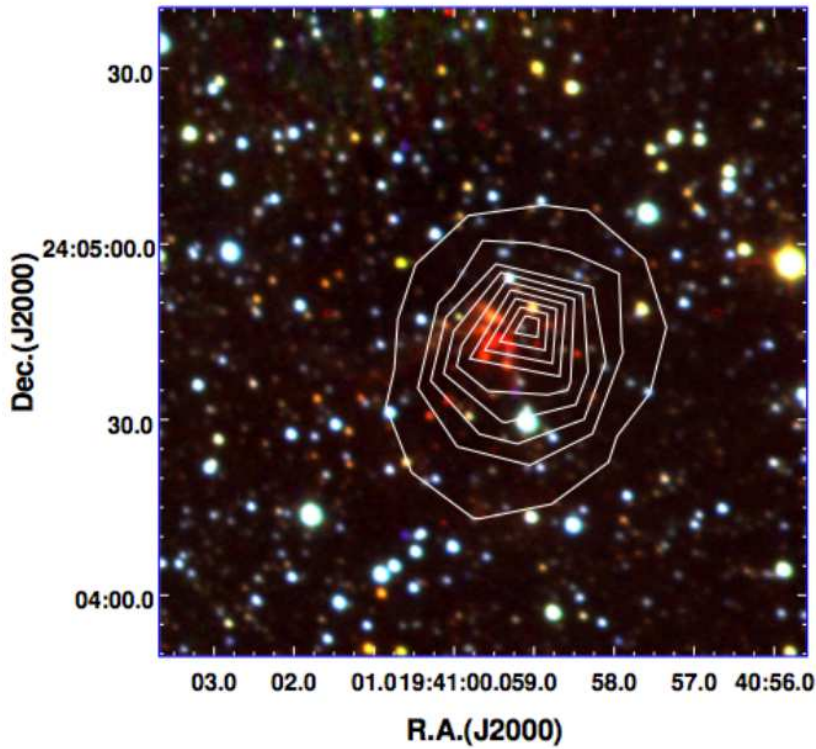


Figure 7: *JHKs* true color image made from *J*(blue), *H*(green) and *Ks* (red) images of IRAS 19388+2357 (Mol 110). The contours represent the Herschel 250 μm emission.

of $167 M_{sun}$ was detected by [20]. The presence of a UCHII region, of water and methanol maser, confirm that Mol110 is an high-mass star forming region.

The IRAS source has been observed in the far-IR as part of the Herschel Infrared Galactic Plane survey (HI-GAL,[21]) at 70, 160, 250, 350, and 500 μm . Figure 7 illustrates our $JHKs$ color coded image with the 250 μm emission overlying. From our near-IR photometry around the IRAS source we have obtained the $J - H$ versus $H - Ks$ diagram.(Fig.8). This shows the presence of a young stellar cluster in the vicinity of IRAS 19388+2357.

Coincident with the IRAS position we have found a source with a strong near-IR excess ($H - Ks=3.36$) and detected also by IRAC/Spitzer. The SED of this source is shown in Fig.6 (*Right panel*) and the relative parameters are reported in Table 2.

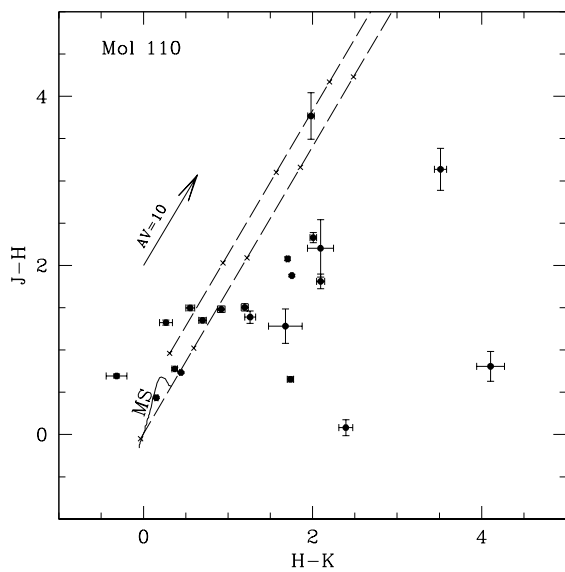


Figure 8: $J - H$ versus $H - Ks$ diagram of IRAS 04579+4703(Mol17)

5. Conclusions

From our near-and mid-IR observations of a sample of high mass young stellar objects we can derive the following conclusions:

- 1) In approximately 63% of our sample we have detected H_2 jets associated to the HMYSOs. In a few cases these are well collimated outflow.
- 2) The analysis of the spectral energy distribution (SED) suggests an accretion disk outflow process in the formation of HMYSOs similar to that observed in low mass young stars, but with an higher mass accretion rate of the order of 10^{-4} to $10^{-3} M_{sun} / \text{year}$. These values are large enough to overcome the radiation pressure from the central star with $L_{bol} \leq 2 \times 10^4 L_{sun}$.
- 3) The objects without any detected outflow in H_2 and without any significant radio emission are likely to be pre-UCHIIs that are in the early stages of their formation.
- 4) Multiple outflows are observed in regions in which are present young stellar clusters .

References

- [1] Varricatt, W.P., Davis, C.J., Ramsay, S., et al. 2010, *MNRAS*, 404 661
- [2] Molinari, S., Brand, J., Cesaroni, R., Palla, F., 1996, *A&A*, 308 587
- [3] Pestalozzi, M.R., Minier, V., Boot, R.S., 2005, *A&A*, 432 737
- [4] Palla, F., Band, J., Cesaroni, R. et al. 1991, *A&A*, 246 249
- [5] Molinari, S., Brand, J., Cesaroni, R., Palla, F., Palumbo, G.G.C., 1998, *A&A*, 336 339
- [6] Molinari, S., Brand, J., Cesaroni, R., Palla, F., 2000, *A&A*, 355 617
- [7] Molinari, S., Testi, L., Rodriguez, L. F., Zhang, Q., 2002, *ApJ*, 570 758
- [8] Zhang, Q., Hunter, T. R., Brand, J., F., et al. 2005, *ApJ*, 625 864
- [9] Hunt, L. H., Mannucci, F., Testi, L. 1998, *AJ*, 115 2594
- [10] Pertsson, S. E., Murphy, D. C., Krzeminiski, W., et al. 1998, *AJ*, 116 2475
- [11] Stetson, P. B., 1987, *PAPS*, 99 191
- [12] Salas, S., Cruz-Gonzales, I., Tapia, M., 2006, *Rev. Mex.Astron. Astrofis*, 42 273
- [13] Xu, J. L., Wang, J. J, Quin, S. L., 2012, *A&A*, 540 L13
- [14] Cesaroni, R., Massi, F., Arcidiacono, C., et al.2015, *A&A*, 581 A124
- [15] Sanchez-Monge, A.,Palau, A., Estalella, R., et al.2008, *A&A*, 485 497
- [16] Wouterloot, J.G.A.,Brand, J., Fiegle, K., 1993, *A&AS*, 98 589
- [17] Robitaille, T. P., Whitney, B. A., Indebetouw, R., et al. 2006, *ApJS*, 167 256
- [18] Robitaille, T. P., Whitney, B. A., Indebetouw, R., Wood, K. 2007,*ApJS* 169 328
- [19] Slysh, V. I.,Valtts, I. E., Kalenskii, S. V., et al. 1999, *A&AS*, 134 115
- [20] Beltran, M. T., Brand, J., Cesaroni, R., et al. 2006, *A&A*, 447 221
- [21] Molinari, S., et al., 2010, *A&A*, 518 L100